医薬品
医薬部外品　研究報告　調査報告書
化粧品

識別番号・報告回数			報告日	第一報入手日	新医薬品等の区分	厚生労働省処理欄
				2005 年 1 月 21 日	該当なし	

一般的名称	①乾燥抗 HBs 人免疫グロブリン ②ポリエチレングリコール処理抗 HBs 人免疫グロブリン	研究報告の公表状況	Science Express Reports, January 20 2005	公表国
販売名（企業名）	①ヘブスブリン（ベネシス） ②静注用ヘブスブリン－IH（ベネシス）			スイス

研究報告の概要

プリオンは通常、神経とリンパ系組織に集積する。炎症性サイトカインと免疫細胞がリンパ系におけるプリオン複製に必要であることから、われわれは今回、炎症条件がプリオンの病態に影響するか否かを調べた。腎臓、膵臓または肝臓に生じる 5 種類の炎症性疾患に罹患したマウスにプリオンを投与したところ、全例で、慢性のリンパ球性炎症により、プリオンが存在しないはずの他の臓器へプリオンが集積していた。また、いずれの炎症の病巣でも、リンフォトキシンの増加ならびに正常な細胞内プリオン蛋白 PrP^{c} を発現する FDC-M1^{+} 細胞の異所性誘導が認められた。他方、リンフォトキシン α またはその受容体を欠損させたマウスの炎症臓器では、異常プリオンである PrP^{sc} の集積は認められず、プリオンを接種しても感染は成立しなかった。したがって、慢性の炎症状態は、プリオンの組織内分布を拡大することによって、自然の、もしくは医原性のプリオン伝播の調節要因として作用すると考えられる。

使用上の注意記載状況・その他参考事項等

代表として静注用ヘブスブリン－IH の記載を示す。
2. 重要な基本的注意
(1)略
1)略
2)現在までに本剤の投与により変異型クロイツフェルト・ヤコブ病（vCJD）等が伝播したとの報告はない。しかしながら、製造工程において異常プリオンを低減し得るとの報告があるものの、理論的な vCJD 等の伝播のリスクを完全には排除できないので、投与の際には患者への説明を十分行い、治療上の必要性を十分検討の上投与すること。

報告企業の意見	今後の対応
プリオンが慢性リンパ球性炎症を起こした臓器に蓄積するとの新たな報告である。 本剤の原料血漿の供給元の米国においてはこれまで固有のvCJD症例は報告されていない。また、これまで血漿分画製剤によってvCJDが伝播したとの報告はない。しかしながら、万一vCJD感染者の血液が本剤の原料に混入した場合には、製造工程においてプリオンを低減し得るとの報告があるものの、製剤から伝播する可能性を完全には否定し得ない。そのため、弊社の血漿分画製剤の製造工程におけるTSE感染性低減に関する検証実験を加速し、自社データを早期に取得し、工程評価を行い、必要に応じて工程改善を実施する。	本報告は本剤の安全性に影響を与えないと考えるので、特段の措置はとらない。

Sciencexpress Report

Chronic Lymphocytic Inflammation Specifies the Organ Tropism of Prions

Mathias Heikenwalder,[1]* Nicolas Zeller,[1]* Harald Seeger,[1]* Marco Prinz,[1]*† Peter-Christian Klöhn,[2] Petra Schwarz,[1] Nancy H. Ruddle,[3] Charles Weissmann,[2] Adriano Aguzzi[1]‡

[1]Institute of Neuropathology, University Hospital of Zürich, CH-8091 Zürich, Switzerland. [2]Medical Research Council Prion Unit, Department of Neurodegenerative Diseases, Institute of Neurology, Queen Square, London WC1N 3BG, UK. [3]Department of Epidemiology and Public Health and Section of Immunobiology, Yale University School of Medicine, New Haven, CT 06520, USA.

*These authors contributed equally to this work.

†Present address: Institute of Neuropathology, Georg-August-Universität, D-37073 Göttingen, Germany.

‡To whom correspondence should be addressed. E-mail: adriano@pathol.unizh.ch

Prions typically accumulate in nervous and lymphoid tissues. Because proinflammatory cytokines and immune cells are required for lymphoid prion replication, we tested whether inflammatory conditions affect prion pathogenesis. We administered prions to mice with five inflammatory diseases of kidney, pancreas or liver. In all cases, chronic lymphocytic inflammation enabled prion accumulation in otherwise prion-free organs. Inflammatory foci consistently correlated with lymphotoxin upregulation and ectopic induction of PrP^C-expressing FDC-M1$^+$ cells, whereas inflamed organs of mice lacking lymphotoxin-α or its receptor did not accumulate PrP^{Sc} nor infectivity upon prion inoculation. By expanding the tissue distribution of prions, chronic inflammatory conditions may act as modifiers of natural and iatrogenic prion transmission.

Although transmissible spongiform encephalopathies selectively damage the central nervous system (CNS), the infectious agent (termed prion) is detectable in lymphoid organs long before clinical symptoms (*1*). PrP^{Sc}, a protease-resistant isoform of the host protein PrP^C, accumulates mostly in CNS and lymphoid organs of infected organisms, and may represent the infectious principle (*2, 3*). In addition to PrP^C (*4*), splenic prion replication requires follicular dendritic cells (FDCs) (*5*), whose maintenance depends on B cells expressing tumor necrosis factor (TNF) and lymphotoxins (LT) α and β (*6–8*). Accordingly, LT/TNF inhibition antagonizes peripheral prion replication (*9–11*). However, most cellular requirements for peripheral prion replication remain unknown (*12*).

Chronic inflammatory conditions present with organized collections of B and T lymphocytes, FDCs, dendritic cells (DCs), as well as marginal-zone and tingible-body macrophages (*13–15*). Extranodal follicles are also prevalent in naturally occurring infections of free-ranging ruminants (*16*). Besides participating in chronic inflammatory conditions, FDCs, B lymphocytes, and other components of the immune system are involved in prion replication (*6–10, 17*). We therefore reasoned that inflammation may affect prion pathogenesis. We studied this question in various transgenic and spontaneous mouse models of chronic inflammation, including nephritis, pancreatitis, and hepatitis.

First, we generated bitransgenic mice expressing LTα and LTβ in liver under the control of the albumin promoter (fig. S1A) (*18, 19*). C57BL/6-Tg(LTab)1222 and C57BL/6-Tg(LTab)1223 mouse lines contained one copy/haploid genome of both AlbLTα and AlbLTβ transgenes (fig. S1B), with expression restricted to liver and absent from thymus, spleen, mesenteric lymph node (MLN), pancreas and kidney (Fig. 1A). C57BL/6-Tg(LTab)1223 mice (henceforth termed AlbLTαβ mice) were identified as the highest expressors (Fig. 1B) and were selected for further experiments.

4-6 month-old AlbLTαβ livers displayed highly organized aggregates of B220$^+$ B lymphocytes, CD3$^+$, CD4$^+$ and CD8$^+$ T cells, FDC-M1$^+$ and CD35$^+$ networks, MOMA-1$^+$ marginal zone-like festoons, CD68$^+$ tingible body macrophages, IgD$^+$ and IgG1$^+$ lymphocytes, ERTR9$^+$ cells, and NLDC-145$^+$ DCs (Fig. 2, A and B) (fig. S1C). AlbLTαβ sinusoids exhibited F4/80$^+$ Kupffer cell hyperproliferation and upregulation of the adhesion molecules I-CAM and V-CAM (fig. S1C). Occasionally, PNA$^+$ clusters indicative of germinal center B cells were found (fig. S1C; arrowheads). None of the above features were found in livers of wild-type littermates (fig. S1C), nor could we detect abnormal histopathological features in AlbLTαβ kidneys, spleens and thymuses.

Transgenic mice expressing LTα under control of the rat insulin promoter (RIP) in pancreatic beta islet cells and renal proximal convoluted tubules (*20–22*) developed interstitial and capsular follicles in kidney and pancreatic islets with

discrete B220$^+$ areas and CD35$^+$/FDC-M1$^+$ networks (*20, 21*) (Fig. 2A). Renal and pancreatic inflammatory foci in RIPLTα and hepatic foci in AlbLTαβ mice were essentially identical in their cellular composition, and expressed various complement components (Fig. 2) (fig. S1D). Splenic and lymph nodal microarchitecture of RIPLTα (n=5), AlbLTαβ (n=3) and wild-type mice (n=3) were indistinguishable upon immunostaining with an exhaustive panel of immunological markers (*23*).

We then studied mice expressing the homeostatic chemokine TCA4/SLC/CCL21 under the control of the rat insulin promoter (*22*). These mice (henceforth termed RIPSLC) contain follicles in the pancreas with organized T and B cell zones, DCs, ER-TR7$^+$ and CD35$^+$ cells, and small FDC-M1$^+$ networks (Fig. 2) (*23*).

NZBxNZW-F_1 (henceforth termed NZBW) and NODLtJ mice are considered models for systemic lupus erythematosus (SLE) and autoimmune diabetes, respectively. NZBW mice develop interstitial nephritis and glomerulonephritis with distinct B and T cell areas, small FDC-M1$^+$ clusters, DCs, small PNA$^+$ clusters and IgG1$^+$ cells (Fig. 2) (fig. S1E). Infiltrates lacked MAdCAM-1$^+$ expression but contained MOMA-1$^+$ cells (fig. S1E). Deposits of C1q, C3, and C4 were identified within glomeruli of kidneys of NZBW mice, but not in parental NZW mice, which did not develop nephritis and were used as controls (Fig. 2) (fig. S1E) (*23*). NODLtJ mice develop spontaneous autoimmune insulitis with lymphoid follicles similar to those developing in NZBW kidneys (*24–26*); NODB10.H2b mice, which do not develop insulitis despite the presence of the NOD locus (*27*), were used as controls.

Real-time RT-PCR analysis of LTα and LTβ expression in inflamed and appropriate control tissues revealed that 6-8 week old AlbLTαβ livers overexpressed LTα ≈45-fold and LTβ 8-10-fold (Fig. 1C). LT expression declined in 8-12 month-old transgenic mice, in parallel with cirrhotic hepatocyte replacement. No other organs of AlbLTαβ mice showed LT overexpression. RIPLTα mice overexpressed LTα and, to a lower extent, LTβ in kidney and pancreas, while RIPSLC mice slightly upregulated LTα expression in pancreas and kidney. LTα and LTβ were strongly upregulated in NODLtJ pancreases, and LTβ was overexpressed in NZBW kidneys and pancreases. In summary, we detected LT upregulation in every instance of chronic inflammation.

RIPLTα, RIPSLC, NZBW, NODLtJ, and isogenic or congenic control mice were inoculated with prions intraperitoneally (10^3 LD_{50}) or intracerebrally ($3x10^2$ LD_{50}). RIPLTα, RIPSLC, and control mice showed similar incubation times and attack rates of disease (Fig. 3A), and the extent of terminal PrP^{Sc} deposition was similar (fig. S2, A and B). Topography and intensity of spongiosis, gliosis, and PrP deposits was found by immunohistochemistry to be similar in brains of all terminally sick mice (*23*). Thus chronic pancreatitis or nephritis did not influence susceptibility to intracerebrally or peripherally administered prions, prion titers, or neuroinvasion speed. Scrapie incubation times of NZBW and NODLtJ mice could not be determined as they exceeded their natural life span. The extent and morphology of inflammation in RIPLTα and RIPSLC kidneys and pancreases, as well as in AlbLTαβ livers, were compared to age-matched mock-infected controls at several time points from 60 days post inoculation (dpi) to terminal disease. We did not detect any modulation of the inflammatory pathologies by prion infection, and intraperitoneal glucose tolerance was unaltered in prion-inoculated RIPLTα mice (fig. S2C).

We then asked whether inflammation influences the distribution of prion infectivity during the preclinical phase of infection. AlbLTαβ, RIPLTα, RIPSLC, NZBW, NZW (8-12 weeks old), NODLtJ, NODB10 (6 months old), and C57BL/6 mice were inoculated i.p. with scrapie prions (5 $logLD_{50}$) and sacrificed at 60, 75, 90 or 100 dpi. Spleen homogenates were assayed for prion infectivity by mouse bioassay (MBA), consisting of intracerebral inoculation of *tga20* indicator mice (*28*) and comparison of scrapie incubation times to a calibration curve (*29*). All spleens displayed comparably high titers of prion infectivity: 4.5-6 (wild-type), 3.5-5 (RIPLTα), 4.2-6.1 (AlbLTαβ), and 3.9-5.7 $logLD_{50}$/g (RIPSLC). Attack rates of indicator mice were 100% at all time points (Fig. 3B). Nephritis and pancreatitis do not affect splenic prion replication.

Prion loads of kidneys, pancreases and livers from prion-infected presymptomatic mice were also determined by MBA (Fig. 3B). Titers were regarded as "borderline" if attack rates were <100%. At 60 dpi, wild-type pancreases and kidneys homogenates lacked measurable infectivity, whereas RIPLTα kidney and pancreas titers ranged between borderline and 1.4 $logLD_{50}$/g. At 75 dpi RIPLTα pancreas and kidney titers were 3.3 or 4 $logLD_{50}$/g, whereas wild-type pancreases and kidneys were non-infectious.

At 90 dpi, all RIPSLC and RIPLTα pancreases and one RIPLTα kidney had prion titers approaching those of spleens (≤3.7 $logLD_{50}$/g in pancreas and ≤2.4$logLD_{50}$/g in kidney), whereas wild-type organs displayed undetectable or borderline infectivity (Fig. 3B). Infectivity of wild-type livers, kidneys, and AlbLTαβ kidneys was borderline or below detectability, whereas AlbLTαβ livers had titers of 3.1-3.4 $logLD_{50}$/g (Fig. 3B). NZBW kidneys were found to contain 2.5-3.5 $logLD_{50}$/g prion infectivity (n=2), whereas NZW kidneys were non-infectious (Fig. 3C).

We subjected organ extracts to scrapie cell assays in end point format (SCEPA) or to conventional scrapie cell assays (SCA), which allow for quantification of prion infectivity

with sensitivity similar to MBAs (*30*). SCEPA and MBA results with RIPLTα homogenates (60 and 90 dpi) were almost completely congruent (fig. S2D and table S1). Wild-type kidneys and pancreases contained no detectable infectivity (<2.54 $logLD_{50}/g$), whereas prion titers in the corresponding RIPLTα extracts were high (table S1). AlbLTαβ liver prion titers (75 dpi) were >3.4$logLD_{50}/g$ tissue in 3/3 liver homogenates, whereas no infectivity was detected in wild-type livers (<2. 4$logLD_{50}/g$) (fig. S2E).

We then administered 5 $logLD_{50}$ scrapie prions i.p. to 6-month old NODLtJ mice and NODB10 mice. Pancreases of hyperglycemic NODLtJ mice contained ≤2 $logLD_{50}/g$ prion infectivity at 50 dpi, whereas control NODB10 mice harbored no or borderline infectivity (Fig. 3D). All *tga20* mice (n=7) that had developed clinical scrapie upon exposure to pancreatic homogenates (50 dpi) displayed spongiosis, gliosis and PrP^{Sc} in immunoblots (figs. S3 and S4), confirming transmission of scrapie infectivity. Similarily, all *tga20* mice that had developed clinical scrapie upon exposure to renal, pancreatic and hepatic homogenates (AlbLTαβ, RIPLTα, RIPSLC, NZBW) showed spongiosis, gliosis and PrP^{Sc} in immunoblots (figs. S3 and S4), confirming transmission of infectivity. However, at 100 dpi (≈10 months of age) pancreatic infectivity was no longer detectable in either genotype, consistently with progressive islet elimination and consecutive regression of pancreatitis in NODLtJ mice (Fig. 3D) (*23*).

We then determined PrP^{Sc} loads in organ extracts. Samples negative by conventional immunoblotting were reanalyzed after phosphotungstate (PTA) precipitation of PrP^{Sc} (*31*), enhancing sensitivity (*32*). At 60, 75 and 90 dpi, PrP^{Sc} was detectable in similar amounts in all spleens of each genotype, but not in livers, kidneys or pancreases of wild-type mice (Fig. 4, A and B). At 60 dpi PrP^{Sc} was undetectable in livers, kidneys or pancreases of any genotype. At 75 dpi we found robust PrP^{Sc} immunoreactivity in 2 of 3 AlbLTαβ livers, but not in RIPLTα kidneys and pancreases (Fig. 4A). At 90 dpi, PrP^{Sc} was readily detectable in all AlbLTαβ livers (Fig. 4A), RIPLTα kidneys, and RIPLTα pancreases (n=6, Fig. 4B). Possible PrP^{Sc} traces were found in one wild-type kidney at 90 dpi (fig. S2F).

PTA-enhanced immunoblot analysis identified PrP^{Sc} in NZBW (n=2) but not in NZW (n=2) kidneys (90 dpi) (Fig. 4C) (*23*). In contrast, PTA-enhanced immunoblotting failed to reveal PrP^{Sc} in NODLtJ and NODB10 pancreases at all time points (50 and 100 dpi), consistent with the low infectivity titers of NODLtJ pancreases at 50 dpi (Fig. 3D).

By which mechanism does inflammation create novel prion reservoirs? PrP^{C} is necessary for prion replication (*4*): hence its expression might be rate-limiting. We thus investigated PrP^{C} expression in wild-type and RIPLTα kidneys and pancreases. Quantitative immunoblot analysis revealed ≤20% increase in total PrP^{C} of RIPLTα kidneys, and no significant changes in transgenic pancreases (fig. S1F). In contrast, immunohistochemical analysis revealed foci of high PrP expression in all analyzed AlbLTαβ livers, RIPLTα kidneys and pancreases, RIPSLC pancreases, NZBW kidneys, and NODLtJ pancreases (Fig. 2B), but not in organs of the appropriate control mice. These foci mostly colocalized with FDC-$M1^{+}$ networks (Fig. 2B).

To characterize the topography of PrP^{Sc} in inflamed prion-infected organs, we assayed (*33*) wild-type, RIPLTα,NZBW and NZW kidneys as well as RIPSLC pancreases by histoblotting. RIPLTα kidneys and pancreases (90 dpi) displayed PrP^{Sc} deposits colocalizing with inflammatory infiltrates, whereas neither feature was found in scrapie-infected wild-type kidneys or pancreases (Fig. 4D). RIPSLC pancreases and NZBW kidneys (90 dpi) also showed small PrP^{Sc} positive areas colocalizing with inflammatory infiltrates, whereas controls were devoid of PrP^{Sc} positive areas (*23*).

Inflammatory conditions cause immune cells to migrate into parenchymal sites of pathology. Some of these immune cells, including activated B lymphocytes, express lymphotoxins which in turn trigger differentiation of FDCs. Lymphotoxin-triggered events, most likely including PrP^{C} upregulation in stromal FDC precursors, appear to confer prion replication competence to sites of inflammation. Lymphotoxin might thus represent a crucial link between inflammation and prion distribution. We tested this prediction by administering prions intraperitoneally to 6-8 month-old $LT\alpha^{-/-}$ and $LT\beta R^{-/-}$ mice, which suffer from spontaneous inflammatory pathologies (*34*), and to age-matched controls. Despite severe multifocal chronic lymphocytic hepatitis with disseminated PNA^{+} clusters (fig. S5, A and B), livers of prion-inoculated $LT\alpha^{-/-}$ and $LT\beta R^{-/-}$ mice were found to be consistently devoid of prion infectivity (fig. S5C) and PrP^{Sc} (fig. S5D).

The above results indicate that chronic follicular inflammation, induced by a variety of causes, specifies prion tropism for otherwise prion-free organs. In most instances infectivity tended to rise with time, suggesting local prion replication. Organ-specific expression of one single pro-inflammatory cytokine (LTα) or chemokine (SLC) sufficed to establish unexpected prion reservoirs, suggesting differentiation of ubiquitous stromal constituents into prion-replication competent cells. In several instances, prion concentration in individual inflamed organs approached that of spleen long before any clinical manifestation of scrapie. Inflamed non-lymphoid organs not only accumulated PrP^{Sc}, but transmitted bona fide prion disease when inoculated into healthy recipient mice.

Knowledge of the distribution of prions within infected hosts is fundamental to consumer protection and prevention

of iatrogenic accidents. Based on the failure to transmit BSE infectivity from any tissue but central nervous system, intestinal, and lymphoid tissue (*35*), the risk to humans of contracting prion infection from other organs has been deemed small even in countries with endemic BSE. It may be important now to test whether superimposed viral, microbial or autoimmune pathologies of farm animals trigger unexpected shifts in the organ tropism of prions. Conversely, the lack of infectivity in "burned out" postinflammatory pancreases suggests that anti-inflammatory regimens may abolish ectopic prion reservoirs.

References and Notes

1. H. Fraser, A. G. Dickinson, *Nature* **226**, 462 (1970).
2. S. B. Prusiner, *Science* **216**, 136 (1982).
3. G. Legname *et al.*, *Science* **305**, 673 (2004).
4. H. R. Büeler *et al.*, *Cell* **73**, 1339 (1993).
5. M. Gonzalez, F. Mackay, J. L. Browning, M. H. Kosco-Vilbois, R. J. Noelle, *J. Exp. Med.* **187**, 997 (1998).
6. T. Kitamoto, T. Muramoto, S. Mohri, K. Doh ura, J. Tateishi, *J. Virol.* **65**, 6292 (1991).
7. K. L. Brown *et al.*, *Nature Med.* **5**, 1308 (1999).
8. M. Prinz *et al.*, *Nature* **425**, 957 (2003).
9. F. Montrasio *et al.*, *Science* **288**, 1257 (2000).
10. N. A. Mabbott, G. McGovern, M. Jeffrey, M. E. Bruce, *J. Virol.* **76**, 5131 (2002).
11. M. Prinz *et al.*, *Proc. Natl. Acad. Sci. U.S.A.* **99**, 919 (2002).
12. A. Aguzzi, *Nature Cell Biol.* **6**, 290 (2004).
13. S. Takemura *et al.*, *J. Immunol.* **167**, 1072 (2001).
14. E. Kaiserling, *Lymphology* **34**, 22 (2001).
15. J. C. Hogg *et al.*, *N. Engl. J. Med.* **350**, 2645 (2004).
16. W. Vernau, R. M. Jacobs, V. E. Valli, J. L. Heeney, *Vet. Pathol.* **34**, 222 (1997).
17. M. A. Klein *et al.*, *Nature Med.* **7**, 488 (2001).
18. R. Magliozzi, S. Columba-Cabezas, B. Serafini, F. Aloisi, *J. Neuroimmunol.* **148**, 11 (2004).
19. See supporting data on *Science* Online.
20. D. E. Picarella, A. Kratz, C. B. Li, N. H. Ruddle, R. A. Flavell, *Proc. Natl. Acad. Sci. U.S.A.* **89**, 10036 (1992).
21. A. Kratz, A. Campos-Neto, M. S. Hanson, N. H. Ruddle, *J. Exp. Med.* **183**, 1461 (1996).
22. L. Fan, C. R. Reilly, Y. Luo, M. E. Dorf, D. Lo, *J. Immunol.* **164**, 3955 (2000).
23. M. Heikenwalder *et al.*, data not shown.
24. A. Hanninen *et al.*, *J. Clin. Invest.* **92**, 2509 (1993).
25. T. L. Delovitch, B. Singh, *Immunity* **7**, 727 (1997).
26. C. Faveeuw, M. C. Gagnerault, F. Lepault, *J. Immunol.* **152**, 5969 (1994).
27. C. P. Robinson *et al.*, *Arthritis Rheum.* **41**, 150 (1998).
28. M. Fischer *et al.*, *EMBO J.* **15**, 1255 (1996).
29. S. B. Prusiner *et al.*, *Ann. Neurol.* **11**, 353 (1982).
30. P. C. Klohn, L. Stoltze, E. Flechsig, M. Enari, C. Weissmann, *Proc. Natl. Acad. Sci. U.S.A.* **100**, 11666 (2003).
31. J. Safar *et al.*, *Nature Med.* **4**, 1157 (1998).
32. J. D. F. Wadsworth *et al.*, *Lancet* **358**, 171 (2001).
33. A. Taraboulos *et al.*, *Proc. Natl. Acad. Sci. U.S.A.* **89**, 7620 (1992).
34. A. Futterer, K. Mink, A. Luz, M. H. Kosco-Vilbois, K. Pfeffer, *Immunity* **9**, 59 (1998).
35. G. A. Wells *et al.*, *Vet. Rec.* **142**, 103 (1998).

36. We thank S. Nedospasov and D. Kuprash for providing LTα/β cDNA, D. Lo for providing Ins-TCA4/SLC mice, C. Sigurdson, G. Miele, M. Zabel, F. Montrasio and M. Le Hir for discussions, as well as A. Gaspert and W. Jochum for histopathological advice, B. Odermatt, R. Moos and G. Bosshard for support with immunohistochemistry and SCA. AA is supported by grants of the Bundesamt für Bildung und Wissenschaft, the Swiss National Foundation, and the NCCR on neural plasticity and repair. MH is supported by the foundation for Research at the Medical Faculty, University of Zurich, a generous educational grant of the Catello family, and a grant of the Verein zur Förderung des akademischen Nachwuchses. PK and CW are supported by the Medical Research Council, UK. NHR is supported by NIH grant NCI R01 CA 16885.

Supporting Online Material
www.sciencemag.cgi/content/full/1106460/DC1
Materials and Methods
Figs. S1 to S5
Table S1
References

18 October 2004; accepted 6 December 2004
Published online 20 January 2005; 10.1126/science.1106460
Include this information when citing this paper.

Fig. 1. Molecular and phenotypic characterization of AlbLTαβ mice. (A) RT-PCR analysis for transgenic LTα, using primers 1 and 2 (see fig. S1A) (450bp), and primers 4 and 5 (see fig. S1A) for transgenic LTβ (390bp) confirmed liver specific transgene expression in AlbLTαβ mice (neg. ctrl.: master mix and H_2O; pos. ctrl.: transgenic plasmid DNA (10ng). (B) Transgene specific real-time RT-PCR analysis identifying C57BL/6-Tg(LTab)1222 as low LTα expressor and C57BL/6-Tg(LTab)1223 as high expressor. (C) Real-time RT-PCR identifying total LTα and LTβ expression in organs of mice with naturally occurring or transgenetically induced inflammatory and autoimmune diseases. Each value represents the fold change ($\log_2$) in individual organs as compared to the average expression in two respective organs of control mice of the appropriate genotype. Each measurement was normalized against β-actin by the ΔΔCt

method. Grey and black symbols denote inflamed and non-inflamed organs, respectively. LTα and/or LTβ were overexpressed not only in LT transgenic organs, but also in inflamed organs of RIPSLC, NZBW and NODLtJ mice.

Fig. 2. Inflammatory foci in AlbLTαβ livers, RIPLTα kidneys, as well as NZBW and RIPSLC pancreases. Consecutive frozen sections of AlbLTαβ liver, RIPSLC pancreas and RIPLTα and NZBW kidneys. **(A)** Follicular inflammatory foci displaying organized collections of B cells (B220) and complement receptor 1-expressing cells (CD35). Scale bar: 200 μm. **(B)** Two-color immunofluorescence analysis. PrP (antiserum XN, red) mainly colocalizes with FDC networks (antibody FDC-M1, green) within follicular infiltrates in all models of follicular inflammation. Scale bar: 20 μm.

Fig. 3. The distribution of PrP^{Sc} and prion infectivity is influenced by inflammatory conditions. **(A)** Survival plots of prion-infected RIPLTαRIPSLC and wild-type (wt) mice, showing similar incubation times after i.p. (RIPLTα:229±10days; wt: 234±6; RIPSLC: 243±8) or i.c. inoculation (RIPLTα:192±2days; wt: 185±6; RIPSLC: 174±2. **(B)** Prion infectivity titers in spleens (circles), pancreases (squares), kidneys (triangles), and livers (crosses) of wild-type (wt) (blue), RIPLTα (red), AlbLTαβ mice (pink) and RIPSLC (green) were determined by transmission to indicator mice at 60, 75 and 90 dpi. Each column lined by vertical dotted lines represents one mouse. Datapoints below the dotted horizontal line indicate attack rates of <100% and were regarded as "borderline infectivity". Error bars were drawn when standard deviation exceeded 0.75 log units. Except for one RIPLTα kidney that elicited an attack rate of 75%, RIPLTα kidneys, pancreases, RIPSLC pancreases and AlbLTαβ livers led to 100% attack rate with high prion titers at 90 dpi. In contrast, wild-type kidneys, pancreases, and livers contained undetectable or at best borderline prion infectivity. (*) One of 4 *tga20* mice died shortly after inoculation. **(C and D)** Prion infectivity titers in kidneys (triangles) of NZW (black), NZBW (brown), NODB10 (orange) and NODLtJ mice (striped) were determined by transmission assay or SCEPA. At 90 dpi NZBW kidneys harbored reasonably high infectivity titers, whereas NZW mice lacked prion infectivity (C). At 50 dpi NODLtJ mice displayed borderline or moderate prion infectivity, whereas NODB10 mice showed no or borderline infectivity. At 100 dpi NODLtJ mice were devoid of detectable prion infectivity, consistently with progressive islet elimination and consecutive regression of pancreatitis (D) (*23*).

Fig. 4. PrP^{Sc} accumulates in inflamed organs of prion-infected mice. **(A)** Immunoblot analysis of liver homogenates after PTA precipitation at 75 (upper blot) and 90 dpi (lower blot). No PrP^{Sc} in 4/4 individual wild-type livers, but clear PrP^{Sc} signal in 4/5 AlbLTαβ livers. Control samples (ctrl.) included undigested healthy brain, PK-digested healthy brain, and PK-digested terminally scrapie-sick brain. PK: Proteinase K, PTA: sodium phosphotungstate precipitation. **(B)** Immunoblot analysis showed strong PrP^{Sc} signal in spleen, kidney and pancreas of prion-infected RIPLTα mice (90 dpi), whereas PrP^{Sc} was confined to spleens of wild-type mice. **(C)** Immunoblot of NZBW and NZW mice. PrP^{Sc} was detected in kidneys of NZBW but not NZW mice. **(D)** Histoblot analysis of prion-infected kidneys. Capsular and subcapsular deposits of PrP^{Sc} co-localize with follicular infiltrates in RIPLTα kidneys. Consecutive sections display colocalization of PrP^{Sc} deposits with follicular infiltrates (H&E).

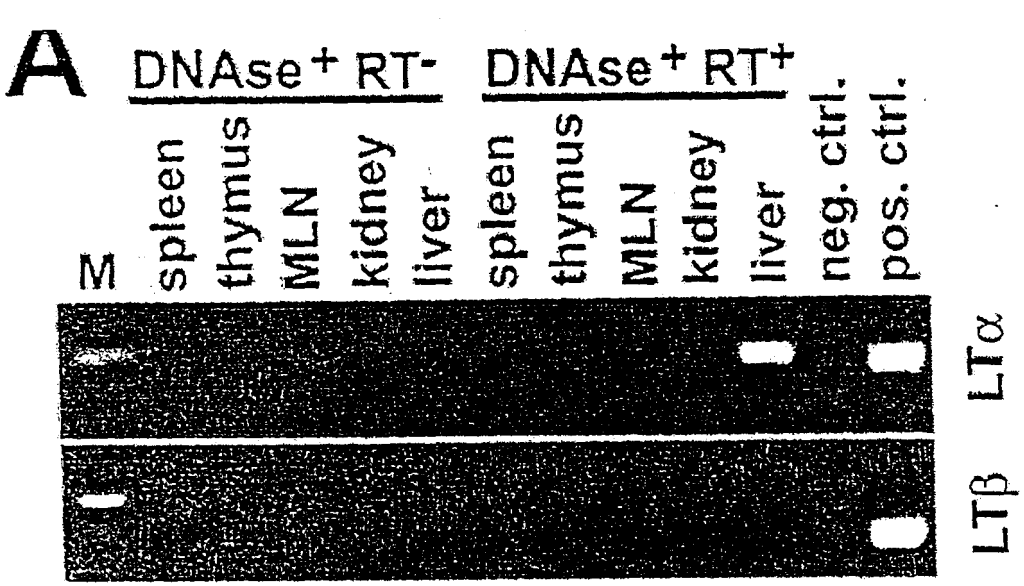
A
DNAse+ RT-
DNAse+ RT+
M
spleen
thymus
MLN
kidney
liver
spleen
thymus
MLN
kidney
liver
neg. ctrl.
pos. ctrl.
LTα
LTβ

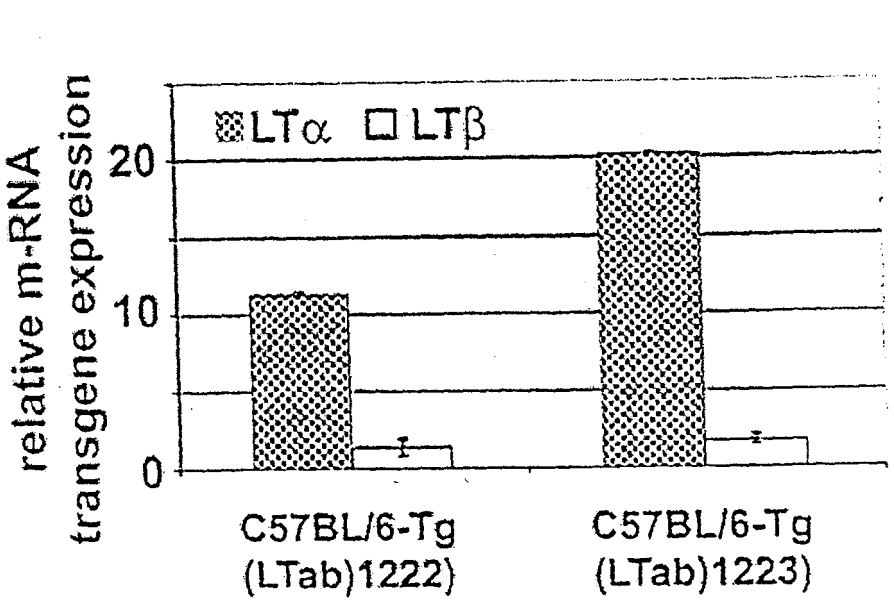
B
LTα
LTβ
relative m-RNA transgene expression
0
10
20
C57BL/6-Tg (LTab)1222)
C57BL/6-Tg (LTab)1223)

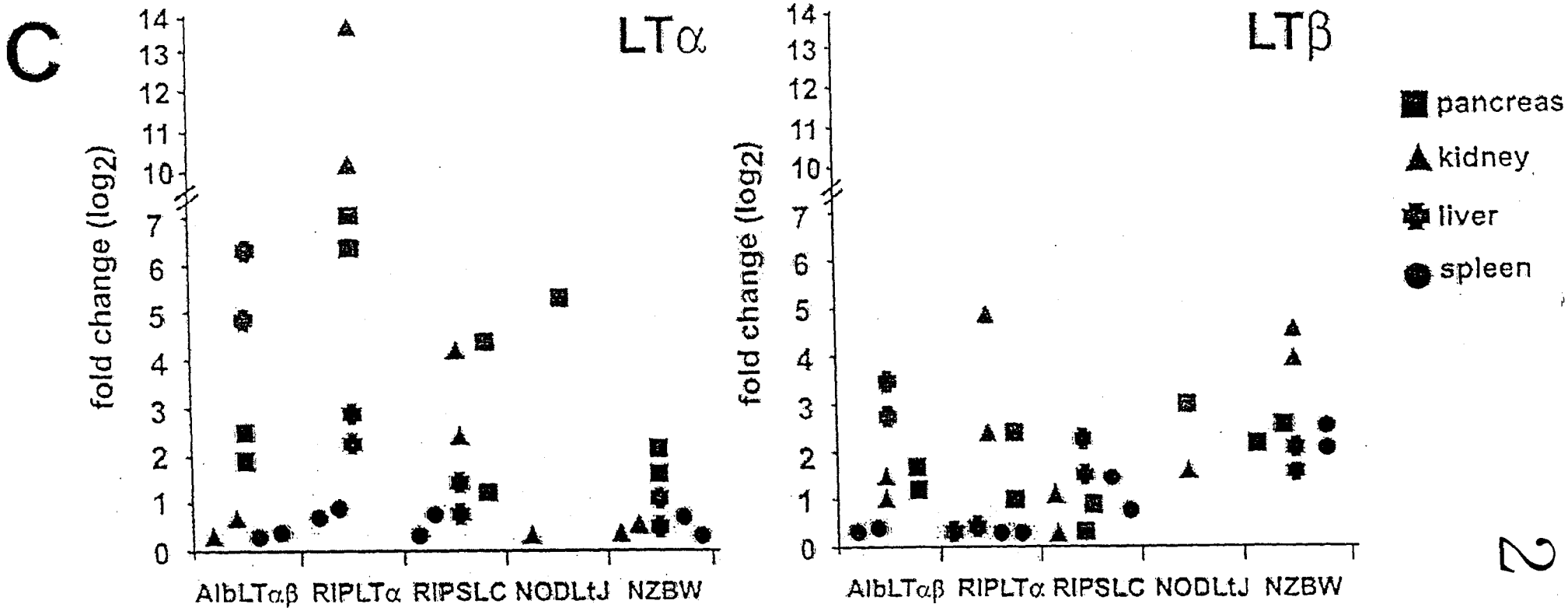
C
LTα
LTβ
fold change (log2)
0
1
2
3
4
5
6
7
10
11
12
13
14
AlbLTαβ
RIPLTα
RIPSLC
NODLtJ
NZBW
pancreas
kidney
liver
spleen

A
B220
CD35
NZBW F1
RIPSLC
RIPLTα
AlbLTαβ
B
FDC-M1
PrP
overlay

survival (%)
i.p. inoculation
LD50
RIPLTα
wt
RIPSLC
i.c. inoculation
wild-typ
RIPLTα
AlbLTα
RIPSLC
NZW
NZBW
NODB10
NODLIJ
spleen
kidney
liver
pancreas
B
transmission assay
prion infectivity titer log LD50
wt
RIPLTα
50 dpi
75 dpi
90 dpi
NODB10
RIPSLC
C
NZW
NZBW F1
D
50 dpi
150 dpi

21

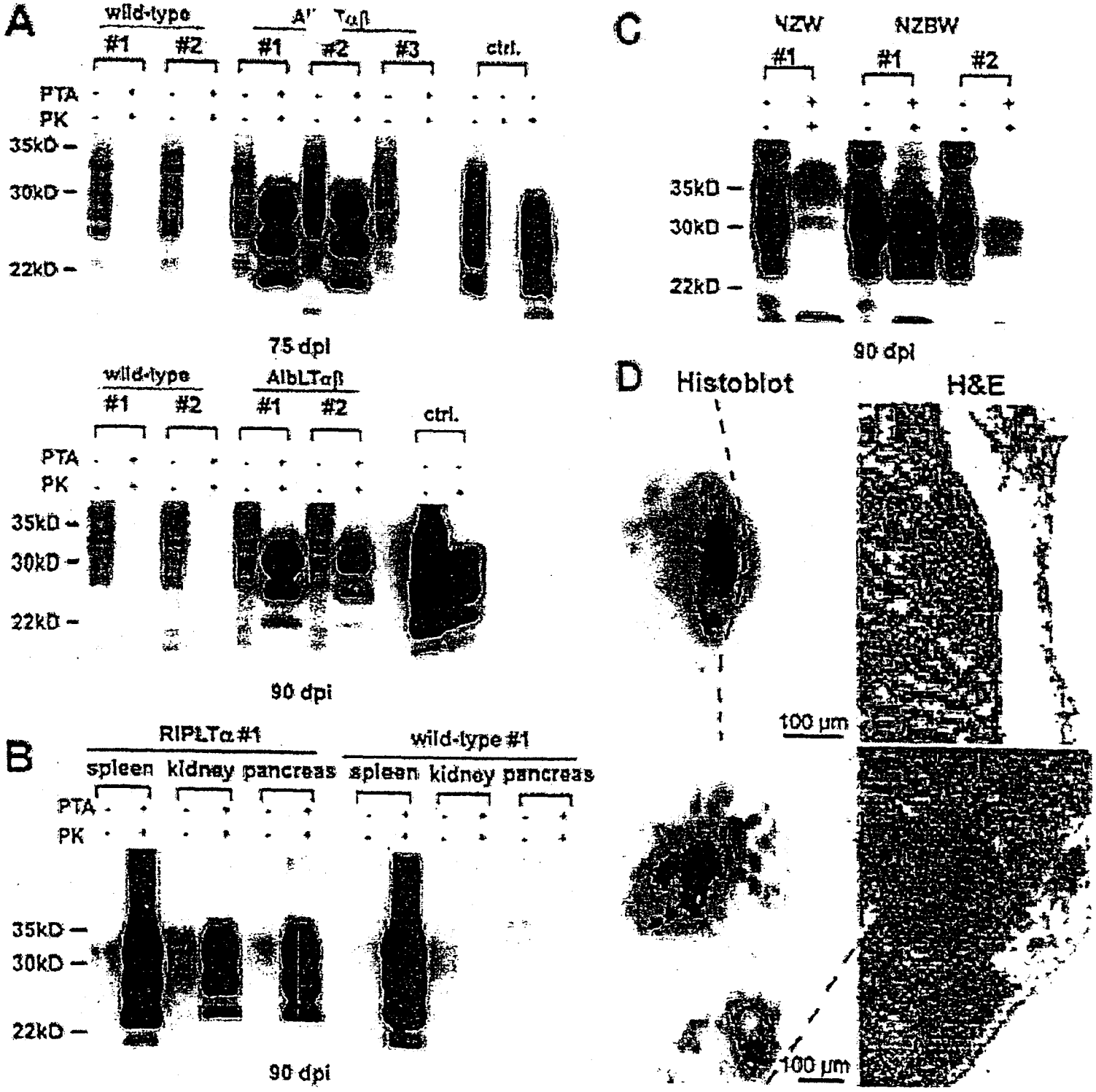
A
wild-type
#1
#2
#1
#2
#3
ctrl.
PTA
PK
35kD
30kD
22kD
75 dpi
wild-type
AlbLTαβ
#1
#2
#1
#2
ctrl.
PTA
PK
35kD
30kD
22kD
90 dpi
B
RIPLTα #1
wild-type #1
spleen
kidney
pancreas
spleen
kidney
pancreas
PTA
PK
35kD
30kD
22kD
90 dpi
C
NZW
NZBW
#1
#1
#2
35kD
30kD
22kD
90 dpi
D
Histoblot
H&E
100 µm
100 µm

21